# Electronic excitation of carbonyl sulphide (COS) by high-resolution vacuum ultraviolet photoabsorption and electron-impact spectroscopy in the energy region from 4 to 11 eV

Journal Item

# Electronic excitation of carbonyl sulphide (COS) by high-resolution vacuum ultraviolet photoabsorption and electron-impact spectroscopy in the energy region from 4 to 11 eV

P. Limão-Vieira, F. Ferreira da Silva, D. Almeida, M. Hoshino, H. Tanaka, D. Mogi, T. Tanioka, N. J. Mason, S. V. Hoffmann, M.-J. Hubin-Franskin, and J. Delwiche

Citation: The Journal of Chemical Physics **142**, 064303 (2015); doi: 10.1063/1.4907200
View online: http://dx.doi.org/10.1063/1.4907200
View Table of Contents: http://aip.scitation.org/toc/jcp/142/6
Published by the American Institute of Physics

# Electronic excitation of carbonyl sulphide (COS) by high-resolution vacuum ultraviolet photoabsorption and electron-impact spectroscopy in the energy region from 4 to 11 eV

P. Limão-Vieira,[1,2,3,a)] F. Ferreira da Silva,[1] D. Almeida,[1] M. Hoshino,[2] H. Tanaka,[2] D. Mogi,[4] T. Tanioka,[5] N. J. Mason,[3] S. V. Hoffmann,[6] M.-J. Hubin-Franskin,[7] and J. Delwiche[7]
[1]*Laboratório de Colisões Atómicas e Moleculares, CEFITEC, Departamento de Física, Faculdade de Ciências e Tecnologia, Universidade Nova de Lisboa, 2829-516 Caparica, Portugal*
[2]*Department of Physics, Sophia University, Tokyo 102-8554, Japan*
[3]*Department of Physical Sciences, The Open University, Walton Hall, Milton Keynes MK7 6AA, United Kingdom*
[4]*Development and Marketing Department, New Products Development Division, Kanto Denka, Kogyo Co., Ltd., Chiyoda-ku, Tokyo 101-0063, Japan*
[5]*Shibukawa Development Research Laboratory, New Products Development Division, Kanto Denka Kogyo Co., Ltd., Shibukawa City, Gunma 377-8513, Japan*
[6]*ISA, Department of Physics and Astronomy, Aarhus University, Ny Munkegade 120, DK-8000 Århus C, Denmark*
[7]*Département de Chimie, Université de Liège, Institut de Chimie-Bât. B6C, allée de la Chimie 3, B-4000 Liège 1, Belgium*

(Received 9 December 2014; accepted 16 January 2015; published online 10 February 2015)

The electronic state spectroscopy of carbonyl sulphide, COS, has been investigated using high resolution vacuum ultraviolet photoabsorption spectroscopy and electron energy loss spectroscopy in the energy range of 4.0–10.8 eV. The spectrum reveals several new features not previously reported in the literature. Vibronic structure has been observed, notably in the low energy absorption dipole forbidden band assigned to the $(4\pi \leftarrow 3\pi)$ $(^1\Delta \leftarrow {}^1\Sigma^+)$ transition, with a new weak transition assigned to $(^1\Sigma^- \leftarrow {}^1\Sigma^+)$ reported here for the first time. The absolute optical oscillator strengths are determined for ground state to $^1\Sigma^+$ and $^1\Pi$ transitions. Based on our recent measurements of differential cross sections for the optically allowed ($^1\Sigma^+$ and $^1\Pi$) transitions of COS by electron impact, the optical oscillator strength $f_0$ value and integral cross sections (ICSs) are derived by applying a generalized oscillator strength analysis. Subsequently, ICSs predicted by the scaling are confirmed down to 60 eV in the intermediate energy region. The measured absolute photoabsorption cross sections have been used to calculate the photolysis lifetime of carbonyl sulphide in the upper stratosphere (20–50 km). © *2015 AIP Publishing LLC.* [http://dx.doi.org/10.1063/1.4907200]

## I. INTRODUCTION

Sulphur compounds are precursors of sulphate aerosol particles and cloud condensation nuclei over remote parts of the oceans which can act as a feedback mechanism in climate regulation by influencing the Earth's radiative balance by direct scattering of solar radiation.[1] The present work is part of a wider research programme aimed at understanding the spectroscopy of sulphur-containing species and the role of these gases in atmospheric chemistry and physics (see, e.g., Refs. 2–4). In order to model these processes in the stratosphere and troposphere, absolute photoabsorption cross sections (oscillator strengths) of such compounds are needed as well as a detailed knowledge of their electronic state spectroscopy.

Carbonyl sulphide (COS) has attracted considerable interest from the international scientific community regarding its role in the Earth's global atmospheric sulphur cycle[5] due to it having both natural[6] and anthropogenic[7] emissions; COS has also been identified as a trace gas in the interstellar medium[8] and identified in other planetary atmospheres.[9] Accordingly, the spectroscopy of COS has been reported in a diverse set of previous works discussing the valence-shell region and the high-energy region. Temperature-dependant photoabsorption cross sections and several electron energy loss studies have been measured and are concisely summarised in Brion's quantitative studies on the photoabsorption of COS in the valence-shell and inner regions (4–360 eV) by dipole electron impact spectroscopies[10] (see Refs. 17-50 in the Introduction).

Wheeler *et al.*[11] reported theoretical calculations on the Renner-Teller bending frequencies of the $\tilde{A}\ ^2\Pi$ state of $COS^+$, whereas the ultraviolet spectrum of COS has been recently investigated by Schmidt and co-workers[12] reporting extensive characteristics of the potential energy surfaces for the two dissociative singlet states calculated at 5.82 and 5.73 eV for the $1^1\Delta$ and $1^1\Sigma^-$, respectively. Ionisation energies (IEs) and vibrational assignments of the lowest-lying ionic states of COS were obtained by high resolution He(I) UV photoelectron spectra of

a)Author to whom correspondence should be addressed. Electronic mail: plimaovieira@fct.unl.pt. Tel.: (+351) 21 294 78 59. Fax: (+351) 21 294 85 49.

 

$COS^+$ by Wang *et al.*[13] including spin-orbit split components in the $\tilde{X}\,^2\Pi$ band. Cossart-Magos[14] reported the absorption spectrum of jet-cooled COS between 64 000 and 91 000 $cm^{-1}$ (7.936–11.284 eV). Finally, a comprehensive and comparative study of elastic electron scattering from COS and $CS_2$ in the energy region from 1.2 to 200 eV has been reported by Murai *et al.*[15] Electronic excitation was investigated by electron impact at 30 and 55 eV by Flicker *et al.*,[16] and thereafter, more extensive studies were performed at 10 and 60 eV electron impact energies and 5–17 eV energy losses with high resolution of 25 meV by Leclerc *et al.*[17] These electron collision studies were focused only on COS spectroscopy, and no reference is made to absolute cross section values. Therefore, to the authors' knowledge, a high-resolution vacuum ultraviolet (VUV) absolute photoabsorption cross section in the 4.0–11 eV energy region has not been reported before. In this paper, we therefore report such a cross section and present a detailed assignment of the valence and Rydberg transitions of neutral COS with new features observed here for the first time.

In Sec. II, we provide a brief summary of the structure and properties of COS, and in Sec. III, we present the experimental details. In addition to identifying the optical electronic transitions of COS, the present work provides reliable photoabsorption cross sections in the range of 4.0–10.8 eV, and through a derivation based on electron energy loss spectroscopy (EELS) results (6.5–9.0 eV), a generalized oscillator strength was determined as in Sec. IV. In Sec. V, the present results are compared with other spectra and absolute photoabsorption cross sections. These photoabsorption cross sections have been used to calculate the photolysis lifetime of carbonyl sulphide in the upper stratosphere (20–50 km). Finally, some conclusions that can be drawn from this study are given in Sec. VI.

## II. BRIEF SUMMARY OF THE STRUCTURE AND PROPERTIES OF CARBONYL SULPHIDE

Carbonyl sulphide is a linear triatomic molecule with $C_{\infty v}$ symmetry, and the electron configuration of the outermost valence orbitals of the $\tilde{X}\,^1\Sigma^+$ ground state is $\ldots(6\sigma)^2\,(7\sigma)^2\,(8\sigma)^2\,(9\sigma)^2\,(2\pi)^4\,(3\pi)^4$ with the three lowest unoccupied molecular orbitals identified as $(4\pi)^0\ (10\sigma)^0\ (11\sigma)^0$.[10] The fundamental vibrational energies (and wave numbers) of COS are 0.107 eV (859 $cm^{-1}$) for the symmetric stretching mode, $\nu_1$, 0.065 eV (520 $cm^{-1}$) for the bending mode, $\nu_2$, and 0.256 eV (2062 $cm^{-1}$) for the antisymmetric stretching mode, $\nu_3$.[18] The electronic transitions excited for the 4.0–10.8 eV photon energy range studies are of the type $(4\pi \leftarrow n\pi)$ yielding $^1\Sigma^+$ and $^1\Delta$; $(10\sigma \leftarrow n\pi)$ and $(11\sigma \leftarrow n\pi)$ yielding $^1\Pi$; and $(10\sigma \leftarrow 8\sigma)$ leading to $^1\Sigma^+$. Transitions from the ground state to the $^1\Sigma^+$ and $^1\Pi$ states are optically allowed.[18] The lowest vertical ionisation energies, which are needed to calculate the quantum defects associated with transitions to Rydberg orbitals, have been identified experimentally by Wang *et al.*[13] using He(I) photoelectron spectroscopy at 11.183 and 11.229 eV $(3\pi)^{-1}$ for $\tilde{X}\,^2\Pi_{3/2}$ and $\tilde{X}\,^2\Pi_{1/2}$, respectively.

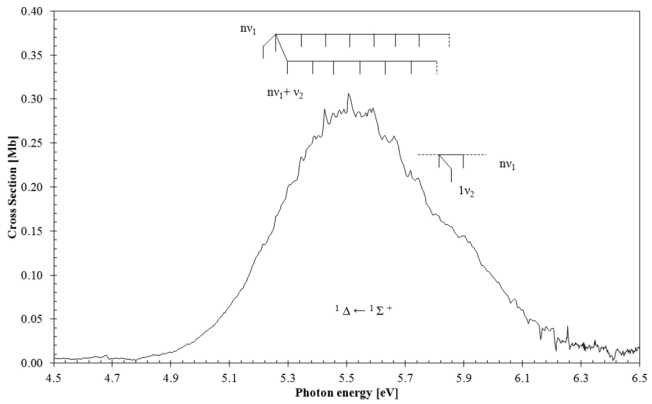


FIG. 2. VUV photoabsorption cross section in the 4.5–6.5 eV absorption band of COS.

## III. EXPERIMENTAL DETAILS

### A. VUV photoabsorption

High-resolution VUV photoabsorption spectra of carbonyl disulphide (Figures 1–6 and Tables I–V for assignments) were recorded using the UV1 beam line of the ASTRID synchrotron facility at the University of Aarhus, Denmark (Figure 1). The experimental apparatus has been described in detail elsewhere[19] so only a brief review will be given here. Briefly, synchrotron radiation passes through a static gas sample and

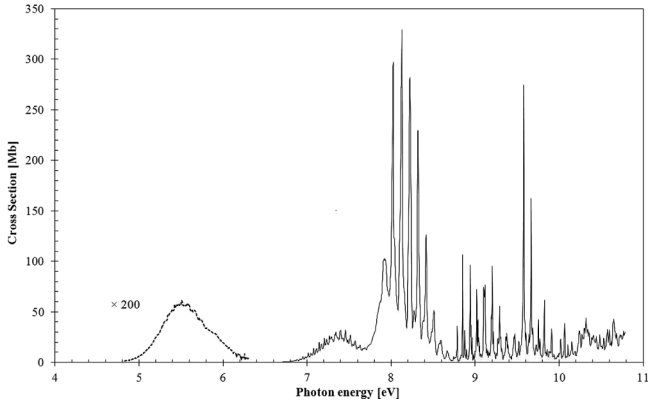


FIG. 1. VUV photoabsorption cross section in the 4.0–11.0 eV absorption band of COS.

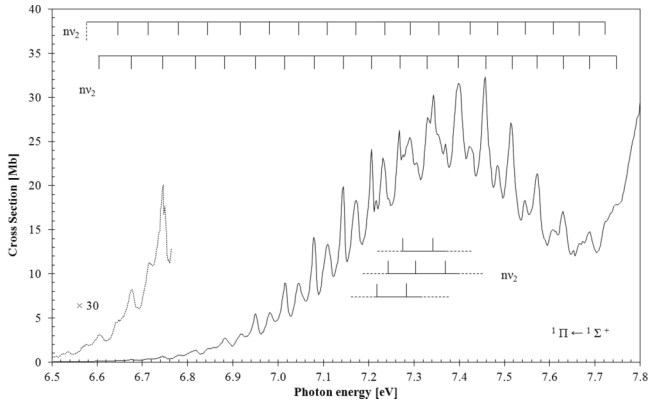


FIG. 3. VUV photoabsorption cross section in the 6.5–7.8 eV absorption band of COS.

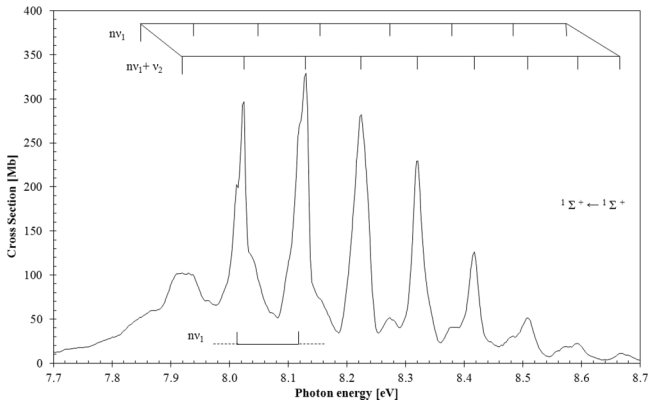


FIG. 4. VUV photoabsorption cross section in the 7.7–8.7 eV absorption band of COS.

a photomultiplier is used to measure the transmitted light intensity. The incident wavelength is selected using a toroidal dispersion grating with 2000 lines/mm providing a resolution of 0.075 nm, corresponding to 3 meV at the midpoint of the energy range studied. For wavelengths below 200 nm (energies above 6.20 eV), helium was flushed through the small gap between the photomultiplier and the exit window of the gas cell to prevent any absorption by molecular oxygen in the air contributing to the spectrum. The sample pressure was measured using a capacitance manometer (Baratron). To ensure that all the data were free of any saturation effects, the absorption cross-sections were measured over the pressure range of 2.67–130.66 Pa (0.02–0.98 Torr), with typical attenuations of less than 10%. The synchrotron beam ring current was monitored throughout the collection of each spectrum, and background scans were recorded with the cell evacuated. Absolute photoabsorption cross sections were then obtained using the Beer-Lambert attenuation law: $I_t = I_0 \exp(-n\sigma x)$, where $I_t$ is the radiation intensity transmitted through the gas sample, $I_0$ is that through the evacuated cell, $n$ the molecular number density of the sample gas, $\sigma$ the absolute photoabsorption cross section, and $x$ the absorption path length (25 cm). The accuracy of the cross section is estimated to be ±5%. Only when absorption by the sample is very weak ($I_0 \approx I_t$), does the error increase as a percentage of the measured cross section.

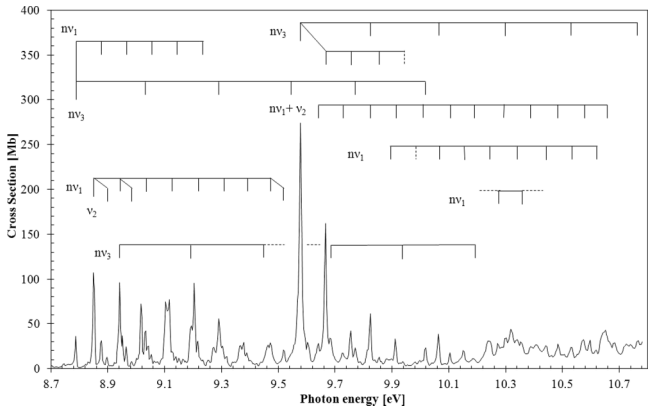


FIG. 5. VUV photoabsorption cross section in the 8.7–10.8 eV absorption band of COS.

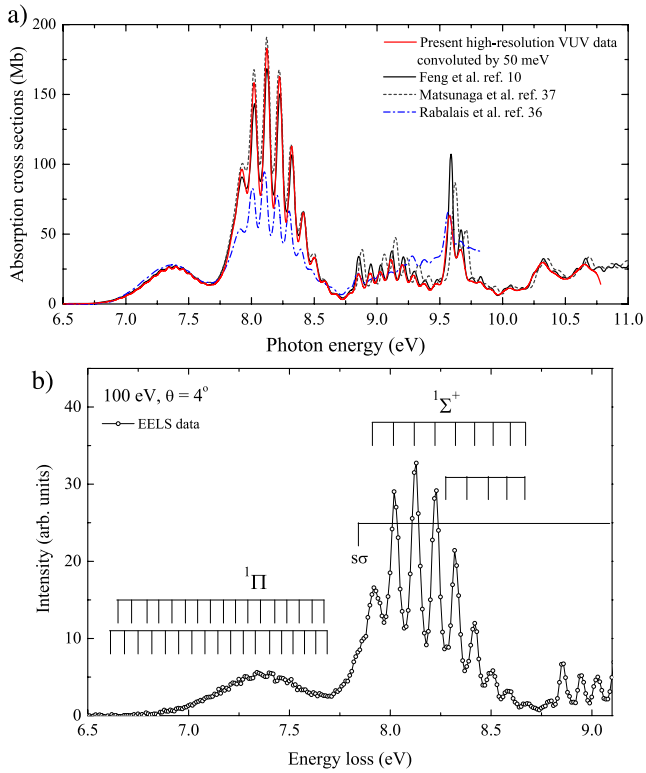


FIG. 6. (a) Comparison of the present absolute photoabsorption cross sections of COS with data published previously; (b) electron energy loss spectrum of COS at 100 eV electron impact and 4° scattering angle.

## B. Electron energy loss spectroscopy

The electron energy loss spectrometer used in this work has been described several times before.[20–22] Briefly, the system is of a crossed electron-molecular beam type with hemispherical monochromator and analyser, differentially pumped, with a set of electron lens system controlled by

TABLE I. Energy values for the vibrational assignments in the $^1\Delta\ (v_1', v_2', 0) \leftarrow \tilde{X}^1\Sigma^+\ (0,0,0)$ absorption band of COS. (b) means a broad feature; (w) weak structure (the last decimal of the energy value is given in brackets for these less-resolved features).

| Energy (eV) | Assignment | ΔE($v_1'$) (eV) | ΔE($v_1'$) (eV) | ΔE($v_2'$) (eV) |
|---|---|---|---|---|
| 5.21(8) (b) | $1v_2'$ | … | … | 0.049 |
| 5.267 | $v_{00}$ | … | … | … |
| 5.312 | $1v_2'$ | … | … | 0.045 |
| 5.349 | $1v_1'$ | 0.081 | … | … |
| 5.391 | $1v_2' + 1v_1'$ | … | 0.079 | … |
| 5.424 | $2v_1'$ | 0.075 | … | … |
| 5.452 | $1v_2' + 2v_1'$ | … | 0.061 | … |
| 5.506 | $3v_1'$ | 0.082 | … | … |
| 5.535 | $1v_2' + 3v_1'$ | … | 0.083 | … |
| 5.579 | $4v_1'$ | 0.073 | … | … |
| 5.630 | $1v_2' + 4v_1'$ | … | 0.095 | … |
| 5.661 | $5v_1'$ | 0.082 | … | … |
| 5.718 | $1v_2' + 5v_1'$ | … | 0.088 | … |
| 5.73(5) (b) | $6v_1'$ | 0.074 | … | … |
| 5.810 | $1v_2' + 6v_1'$ | … | 0.092 | … |
| 5.84(3) (w) | $7v_1'$ | 0.108 | … | … |

TABLE II. Energy values for the vibrational assignments in the $^1\Pi$ (0,$\nu'_2$,0) $\leftarrow \tilde{X}\,^1\Sigma^+$ (0,0,0) absorption band of COS. (w) means weak structure; (b) a broad feature; (s) indicates a shoulder (the last decimal of the energy value is given in brackets for these less-resolved features).

| Energy (eV) | Assignment | $\Delta E(\nu'_2)$ (eV) | Assignment | $\Delta E(\nu'_2)$ (eV) |
|---|---|---|---|---|
| 6.57(4) (w) | $\nu_{00}$ | ... | ... | ... |
| 6.602 | ... | ... | ... | ... |
| 6.643 | $1\nu'_2$ | 0.069 | ... | ... |
| 6.678 | ... | ... | $1\nu'_2$ | 0.076 |
| 6.716 | $2\nu'_2$ | 0.073 | ... | ... |
| 6.746 | ... | ... | $2\nu'_2$ | 0.068 |
| 6.781 | $3\nu'_2$ | 0.065 | ... | ... |
| 6.818 | ... | ... | $3\nu'_2$ | 0.072 |
| 6.844 | $4\nu'_2$ | 0.063 | ... | ... |
| 6.882 | ... | ... | $4\nu'_2$ | 0.064 |
| 6.919 | $5\nu'_2$ | 0.075 | ... | ... |
| 6.950 | ... | ... | $5\nu'_2$ | 0.068 |
| 6.982 | $6\nu'_2$ | 0.064 | ... | ... |
| 7.015 | ... | ... | $6\nu'_2$ | 0.065 |
| 7.047 | $7\nu'_2$ | 0.064 | ... | ... |
| 7.079 | ... | ... | $7\nu'_2$ | 0.064 |
| 7.109 | $8\nu'_2$ | 0.062 | ... | ... |
| 7.144 | ... | ... | $8\nu'_2$ | 0.065 |
| 7.173 | $9\nu'_2$ | 0.064 | ... | ... |
| 7.206 | ... | ... | $9\nu'_2$ | 0.062 |
| 7.231 | $10\nu'_2$ | 0.058 | ... | ... |
| 7.268 | ... | ... | $10\nu'_2$ | 0.062 |
| 7.291 | $11\nu'_2$ | 0.060 | ... | ... |
| 7.330 | ... | ... | $11\nu'_2$ | 0.062 |
| 7.354 | $12\nu'_2$ | 0.063 | ... | ... |
| 7.39(9) (b) | ... | ... | $12\nu'_2$ | 0.069 |
| 7.422 | $13\nu'_2$ | 0.068 | ... | ... |
| 7.458 | ... | ... | $13\nu'_2$ | 0.059 |
| 7.485 | $14\nu'_2$ | 0.063 | ... | ... |
| 7.514 | ... | ... | $14\nu'_2$ | 0.056 |
| 7.546 | $15\nu'_2$ | 0.061 | ... | ... |
| 7.574 | ... | ... | $15\nu'_2$ | 0.060 |
| 7.606 | $16\nu'_2$ | 0.060 | ... | ... |
| 7.630 | ... | ... | $16\nu'_2$ | 0.059 |
| 7.668 | $17\nu'_2$ | 0.062 | ... | ... |
| 7.689 | ... | ... | $17\nu'_2$ | 0.059 |
| 7.72(5) (s) | $18\nu'_2$ | 0.057 | ... | ... |
| 7.749 | ... | ... | $18\nu'_2$ | 0.060 |
| 7.217 | ... | ... | | |
| 7.28(3) (s) | $1\nu'_2$ | 0.066 | | |
| 7.24(4) (s) | ... | ... | | |
| 7.306 | $1\nu'_2$ | 0.062 | | |
| 7.369 | $2\nu'_2$ | 0.063 | | |
| 7.276 | ... | ... | | |
| 7.343 | $1\nu'_2$ | 0.067 | | |

TABLE III. Energy values for the vibrational assignments in the $^1\Sigma^+$ ($\nu'_1$,$\nu'_2$,0) $\leftarrow \tilde{X}\,^1\Sigma^+$ (0,0,0) absorption band of COS. (w) means weak structure; (b) a broad feature; (s) indicates a shoulder (the last decimal of the energy value is given in brackets for these less-resolved features).

| Energy (eV) | Assignment | $\Delta E(\nu'_1)$ (eV) | Assignment | $\Delta E(\nu'_1)$ (eV) |
|---|---|---|---|---|
| 7.85(2) (b) | $\nu_{00}$ | ... | ... | ... |
| 7.92(0) (b) | ... | ... | $1\nu'_2$ | ... |
| 7.93(8) (b) | $1\nu'_1$ | 0.086 | ... | ... |
| 8.025 | ... | ... | $1\nu'_2+1\nu'_1$ | 0.105 |
| 8.04(6) (s) | $2\nu'_1$ | 0.108 | ... | ... |
| 8.130 | ... | ... | $1\nu'_2+2\nu'_1$ | 0.105 |
| 8.15(4) (s) | $3\nu'_1$ | 0.108 | ... | ... |
| 8.224 | ... | ... | $1\nu'_2+3\nu'_1$ | 0.094 |
| 8.274 | $4\nu'_1$ | 0.120 | ... | ... |
| 8.321 | ... | ... | $1\nu'_2+4\nu'_1$ | 0.097 |
| 8.37(7) (b) | $5\nu'_1$ | 0.103 | ... | ... |
| 8.417 | ... | ... | $1\nu'_2+5\nu'_1$ | 0.096 |
| 8.48(3) (s) | $6\nu'_1$ | 0.106 | ... | ... |
| 8.510 | ... | ... | $1\nu'_2+6\nu'_1$ | 0.093 |
| 8.57(4) (s) | $7\nu'_1$ | 0.091 | ... | ... |
| 8.595 | ... | ... | $1\nu'_2+7\nu'_1$ | 0.085 |
| 8.664 | ... | ... | $1\nu'_2+8\nu'_1$ | 0.069 |
| 8.012 | ... | ... | | |
| 8.11(7) (s) | $1\nu'_1$ | 0.105 | | |

computer-driven voltages. The experimental setup was operated at impact energies from 60 to 300 eV and scattering angles from 2° to 20°, with typical energy resolution of 45–55 meV at full width at half maximum (FWHM), which is generally speaking constant throughout the energy range. The electron energy scale was calibrated against the 19.37 eV Feshbach resonance in He. The angular scale and resolution (3.0° (FWHM)) were determined from the symmetry in the intensity profile of the He $2^1$P excitation measured at the 0° nominal-scattering angle. The molecular beam was produced effusively from a nozzle with a 5 mm length and 0.3 mm in diameter. The observed elastic scattered electrons were converted into absolute cross sections by using the standard relative flow technique with He differential cross sections (DCSs) as the reference species.[23] For a comprehensive description of this technique see Refs. 24–26. This implies adjustment of the relative gas (COS, He) pressures to ensure their Knudsen numbers are approximately equal, so that the gas beam profiles remain similar. The actual head pressures behind the nozzle were about 0.5 Torr for COS and 3.0 Torr for He. To place the absolute scale into the inelastic DCSs, the measured energy loss spectra are normalized to the absolute elastic DCS.

### C. COS sample

The gas sample used in the VUV photoabsorption experiment was purchased from Sigma-Aldrich with a stated purity of ≥97.5%, whereas in the EELS experiment was purchased from Kanto Denka Kogyo Co., Ltd., with a stated purity of 99.9%. The sample was used as delivered in both setups.

## IV. FITTING PROCEDURES

The corresponding integral cross sections obtained through electron scattering from COS were derived by applying a generalized oscillator strength analysis and then assessed against the *BE* (Binary-encounter) and *f* scaling. The values of the DCS ($E_0$, θ) for the intense optically allowed transition (3π → 10σ) $^1\Pi$ are transformed to the experimental generalized oscillator strength, $GOS_{\text{expt}}$ through[27]

$$GOS_{\text{expt}}(K^2) = \frac{(E/R)k_i a_0}{4a_0^2 k_f a_0} K^2 DCS(E_0, \theta), \qquad (1)$$

TABLE IV. Energy values for the vibrational assignments in the $\tilde{E}\,^1\Pi\ (v'_1,0,v'_3) \leftarrow \tilde{X}\,^1\Sigma^+\ (0,0,0)$, and $\tilde{F}\,^1\Pi\ (v'_1,v'_2,v'_3) \leftarrow \tilde{X}\,^1\Sigma^+\ (0,0,0)$ absorption bands of COS. (w) means weak structure; (b) a broad feature; (s) indicates a shoulder (the last decimal of the energy value is given in brackets for these less-resolved features).

| Energy (eV) | Assignment | $\Delta E(v'_1)$ (eV) | Assignment | $\Delta E(v'_3)$ (eV) |
|---|---|---|---|---|
| 8.787 | $v_{00}$ | ... | ... | ... |
| 8.878 | $1v'_1$ | 0.091 | ... | ... |
| 8.965 | $2v'_1$ | 0.087 | ... | ... |
| 9.033 | ... | ... | $1v'_3$ | 0.246 |
| 9.053 | $3v'_1$ | 0.088 | ... | ... |
| 9.140 | $4v'_1$ | 0.087 | ... | ... |
| 9.291 | ... | - | $2v'_3$ | 0.258 |
| 9.235 | ... | 0.095 | ... | ... |
| 9.559 | ... | ... | $3v'_3$ | 0.268 |
| 9.770 | ... | ... | $4v'_3$ | 0.211 |
| 10.019 | ... | ... | $5v'_3$ | 0.249 |
| **Energy (eV)** | **Assignment** | **$\Delta E(v'_1)$ (eV)** | **Assignment** | **$\Delta E(v'_3)$ (eV)** |
| 8.850 | $v_{00}$ | ... | ... | ... |
| 8.942 | $1v'_1$ | 0.092 | ... | ... |
| 9.033 | $2v'_1$ | 0.091 | ... | ... |
| 9.12(6) (s) | $3v'_1$ | 0.093 | ... | ... |
| 9.194 | ... | ... | $1v'_1 + 1v'_3$ | 0.252 |
| 9.218 | $4v'_1$ | 0.092 | ... | ... |
| 9.305 | $5v'_1$ | 0.087 | ... | ... |
| 9.389 | $6v'_1$ | 0.084 | ... | ... |
| 9.44(4) (s) | ... | ... | $1v'_1 + 2v'_3$ | 0.260 |
| 9.472 | $7v'_1$ | 0.083 | ... | ... |
| 9.68(3) (s) | ... | ... | $1v'_1 + 3v'_3$ | 0.229 |
| 9.93(9) (w) | ... | ... | $1v'_1 + 4v'_3$ | 0.256 |
| 10.18(8) (b) | ... | ... | $1v'_1 + 5v'_3$ | 0.249 |
| **Energy (eV)** | **Assignment** | **$\Delta E(v'_2)$ (eV)** | | |
| 8.850 | ... | ... | | |
| 8.897 | $1v'_2$ | 0.047 | | |
| 8.942 | ... | ... | | |
| 8.984 | $1v'_2$ | 0.042 | | |
| 9.472 | ... | ... | | |
| 9.519 | $1v'_2$ | 0.047 | | |

where $k_i$ and $k_f$ are the initial and final momenta of the incident electron, $a_0$ is the Bohr radius (0.529 Å), $R$ is the Rydberg constant (13.61 eV), $E_0$ is the energy of the incident electron, $E$ is the excitation energy, and $GOS_{expt}$ $(K^2)$ is the experimental GOS, and $K^2$ is the momentum transfer squared defined by

$$Ka^2 = (k_i a_0)^2 + (k_f a_0)^2 - 2(k_i a_0)(k_f a_0)\cos\theta. \quad (2)$$

The experimental data are fitted with a semi-theoretical formula proposed by Vriens[28] for a dipole-allowed excitation

$$G(x) = \frac{1}{(1+x)^6}\left[\sum_{m=0}^{\infty}\frac{f_m x^m}{(1+x)^m}\right], \quad (3)$$

where

$$x = \frac{K^2}{\alpha^2} \quad (4)$$

and

$$\alpha = \sqrt{\frac{B}{R}} + \sqrt{\frac{B-E}{R}}, \quad (5)$$

with $B$ being the binding energy of the target electron being excited. In Eq. (3), the $f_m$ values are fitting constants to be determined in a least-squares fit analysis of the experimental GOSs ($G_{expt}$), as from Figures 7(a) and 7(b). The experimental optical oscillator strengths (OOSs) can now be extracted from the $f_0$ coefficient that was determined from the fit in each case, as $K \to 0$ (Lassettre limit theorem[29]). A comparison of the $f_0$ values with those derived from the photoabsorption data shows another assessment for verification and validation of the measurements as shown in Table VI. The present $f_0$ values, 0.59 for $^1\Sigma^+$ and 0.13 for $^1\Pi$, obtained by photoabsorption as well as by electron impact spectroscopy agree perfectly well with the OOS value of 0.60 for $^1\Sigma^+$ and 0.13 for $^1\Pi$ reported in Brion and co-workers.[10] An estimation of the ICS, at each energy, can be obtained from Eqs. (3)–(5) using the standard formulation as in Ref. 30 by integrating $G_{expt}(K^2)$ over the limits of $K^2$ corresponding to $\theta = 0°$ and 180°,

$$ICS_{expt}(E_0) = \frac{4\pi a_0^2}{E_0/R}\int_{K^2\,min}^{K^2\,max}\frac{G_{expt}(K^2)}{E/R}d(\ell n K^2), \quad (6)$$

with

$$K^2{}_{min} = 2\frac{E_0}{R}\left[1 - \frac{E}{2E_0} - \sqrt{1-\frac{E}{E_0}}\right] \quad (7)$$

and

$$K^2{}_{max} = 2\frac{E_0}{R}\left[1 - \frac{E}{2E_0} + \sqrt{1-\frac{E}{E_0}}\right]. \quad (8)$$

The results for the $^1\Pi$ and $^1\Sigma^+$ electronic states are plotted in Figures 8(a) and 8(b). This is discussed in more detail in Sec. V C.

### A. BE*f*-scaling method

Scaled (plane wave) Born cross sections for dipole-allowed excitations-$f$-scaling and BE-scaling, and BE$f$-scaling have been described in detail by Kim in Ref. 31 so only a brief description is given for the points relevant to the present study. The Born approximation gives fairly good agreement for the excitation cross section in optically allowed transitions at high collision-energies, whilst a modified simple scaling method for the excitation cross section of atoms, and also extended for the case of molecular targets, over the entire range of collision energies was proposed by Kim.[31] As so, the BE$f$-scaled Born cross section, $\sigma_{BEf}$, is given by

$$\sigma_{BEF}(E_0) = \frac{f_{accur}E_0}{f_{Born}(E_0 + B + E)}\sigma_{Born}(E_0), \quad (9)$$

where $f_{accur}$ is an accurate value obtained from experiments (photoabsorption) or calculations with accurate wave functions, and $f_{Born}$ is the value from the calculation with the wave function employed in the calculation of the unscaled Born

TABLE V. Energy values for the vibrational assignments in 9.5–10.8 eV absorption region of COS. (w) means weak structure; (b) a broad feature (the last decimal of the energy value is given in brackets for these less-resolved features).

| Energy (eV) | Assignment | $\Delta E(\nu_1')$ (eV) | Assignment | $\Delta E(\nu_3')$ (eV) | Assignment | | |
|---|---|---|---|---|---|---|---|
| 9.578 | $\nu_{00}$ | … | … | … | … | … | … |
| 9.641 | … | … | … | … | $1\nu_2'$ | … | … |
| 9.667 | $1\nu_1'$ | 0.089 | … | … | … | … | … |
| 9.724 | … | … | … | … | $1\nu_2'+1\nu_1'$ | … | … |
| 9.755 | $2\nu_1'$ | 0.088 | … | … | … | … | … |
| 9.824 | … | … | $1\nu_3'$ | 0.246 | $1\nu_2'+2\nu_1'$ | … | … |
| 9.856 | $3\nu_1'$ | 0.101 | … | … | … | … | … |
| 9.88(3) (w) | … | … | … | … | | $\nu_{00}$ | … |
| 9.911 | $4\nu_1'$ | … | … | … | $1\nu_2'+3\nu_1'$ | … | … |
| 9.93(8) (w) | … | 0.082 | … | … | … | … | … |
| 9.98(3) (w) | … | … | … | … | … | $1\nu_1'$ | … |
| 10.019 | $5\nu_2'$ | … | … | … | $1\nu_2'+4\nu_1'$ | … | … |
| 10.064 | … | … | $2\nu_3'$ | 0.240 | … | $2\nu_1'$ | … |
| 10.105 | $6\nu_2'$ | … | … | … | $1\nu_2'+5\nu_1'$ | … | … |
| 10.150 | … | … | … | … | … | $3\nu_1'$ | … |
| 10.18(8) (b) | $7\nu_2'$ | … | … | … | $1\nu_2'+6\nu_1'$ | … | … |
| 10.238 | … | … | … | … | … | $4\nu_1'$ | … |
| 10.272 | $8\nu_2'$ | … | … | … | … | … | $1\nu_1'$ |
| 10.30(2) (b) | … | … | $3\nu_3'$ | 0.238 | $1\nu_2'+7\nu_1'$ | … | … |
| 10.341 | $9\nu_2'$ | … | … | … | … | $5\nu_1'$ | … |
| 10.354 | … | … | … | … | … | … | $2\nu_1'$ |
| 10.388 | $10\nu_2'$ | … | … | … | $1\nu_2'+8\nu_1'$ | … | … |
| 10.441 | … | … | … | … | … | $6\nu_1'$ | … |
| 10.485 | $11\nu_2'$ | … | … | … | $1\nu_2'+9\nu_1'$ | … | … |
| 10.529 | … | … | $4\nu_3'$ | 0.227 | … | $7\nu_1'$ | … |
| 10.574 | $12\nu_2'$ | … | … | … | $1\nu_2'+10\nu_1'$ | … | … |
| 10.620 | … | … | … | … | … | $8\nu_1'$ | … |
| 10.64(7) (b) | $13\nu_2'$ | … | … | … | $1\nu_2'+11\nu_1'$ | … | … |
| 10.767 | … | … | $5\nu_3'$ | 0.238 | … | … | … |

cross section $\sigma_{\text{Born}}$. In the present study, however, we have employed our own experimental high energy results as the unscaled $\sigma_{\text{Born}}$ at $E_0$ = 100, 200, and 300 eV in Eq. (9) since no Born calculation was available in the literature. The $f$-scaling process has the effect of correcting the wave function used for $\sigma_{\text{Born}}$ with an accurate value, e.g., an experimental $f_0$ value derived from the present photoabsorption data. Thus, the BE$f$-scaling corrects the deficiency of the Born approximation at low $E_0$, without losing its well-known validity at high $E_0$ values. We have successfully applied this method to atoms and molecules in previous occasions (see, e.g., Refs. 32 and 33). As shown in Figures 8(a) and 8(c), it is found that the BE$f$-scaled Born method generates fairly good values over the collision energies for COS $^1\Pi$ and $^1\Sigma^+$ optically allowed transitions, respectively.

## V. ELECTRONIC STATE SPECTROSCOPY: RESULTS AND DISCUSSION

The absolute high resolution VUV photoabsorption cross section of carbonyl sulphide is shown in Figure 1, extending from 4.0 to 10.8 eV, with detailed sections of the measured cross section being shown in Figures 2–5. The major absorption bands can be classified as a mixture of Rydberg series and molecular valence transitions of the type $(4\pi \leftarrow n\pi)\ ^1\Sigma^+$ and $^1\Delta$; $(10\sigma \leftarrow n\pi)$ and $(11\sigma \leftarrow n\pi)\ ^1\Pi$; and $(10\sigma \leftarrow 8\sigma)\ ^1\Sigma^+$. Tables I–V show the energy values for the vibrational assignments in the different absorption bands of COS. Figure 6(a) shows a comparison of the present absolute photoabsorption cross sections of COS with data published previously.[10] We observe a reasonable agreement between the different sets of data although we note some deviations in the position of some of the absorption features in particular above 8.75 eV. Since there is no numerical data available to compare with, Matsunaga *et al.*[37] and Rabalais *et al.*[36] data have been scanned and added to Feng *et al.*'s in their Figure 6 in Ref. 10. Figure 6(b) shows an electron energy loss spectrum of COS at 100 eV electron impact and 4° scattering angle, whereas in Figures 7 and 8, we display the GOS fitting and ICSs, respectively, for the $^1\Sigma^+$ and $^1\Pi$ states. Absolute oscillator strengths and relative intensities are compared for $^1\Pi$, ns$\sigma$, and $^1\Sigma^+$ states of carbonyl sulphide in Table VI.

### A. Valence state spectroscopy of carbonyl sulphide

The present measurements in the 4.0–10.8 eV energy range below the first ionisation energy confirm the presence of low-lying absorption bands centred at 5.506, 7.458, and 8.130 eV assigned to $(4\pi \leftarrow 3\pi)$ $(^1\Delta \leftarrow {}^1\Sigma^+)$, $(10\sigma \leftarrow 3\pi)$ $(^1\Pi \leftarrow {}^1\Sigma^+)$, and $(4\pi \leftarrow 3\pi)$ $(^1\Sigma^+ \leftarrow {}^1\Sigma^+)$ and in very good

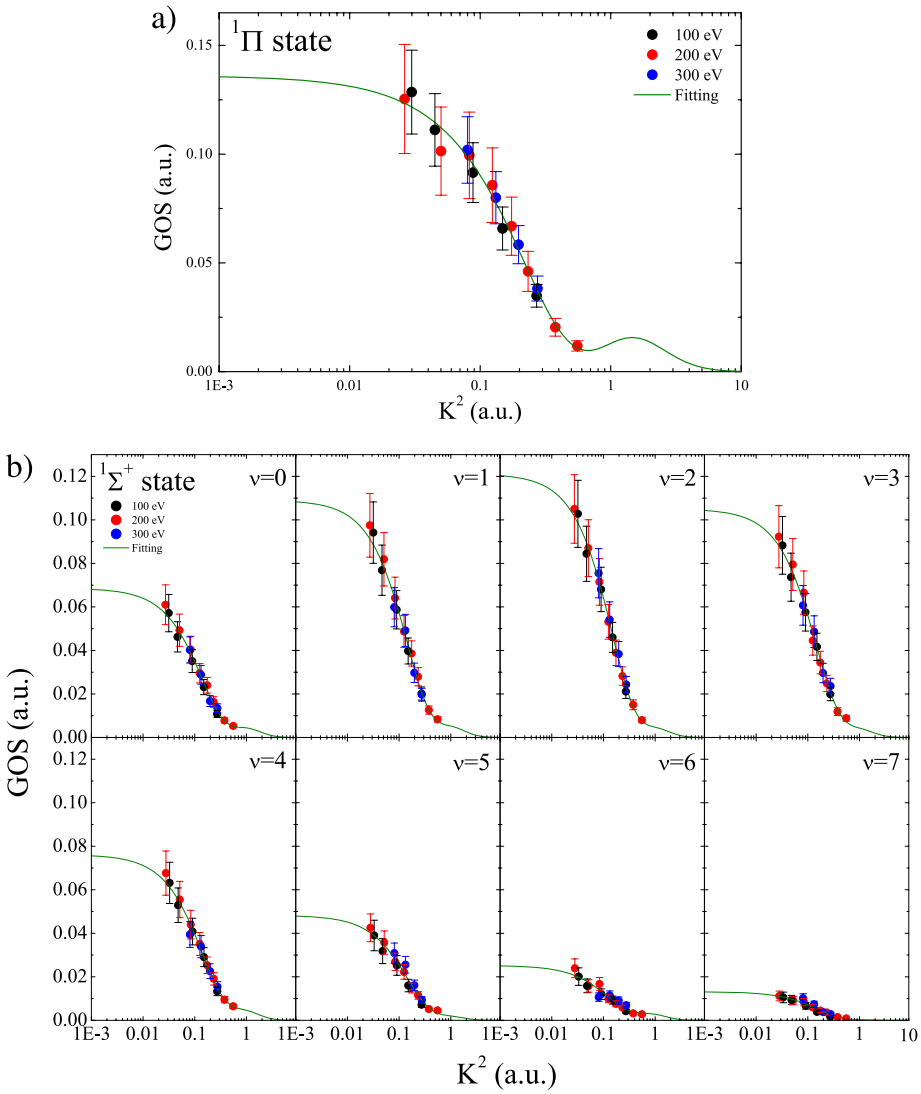


FIG. 7. Generalised oscillator strengths for COS electron impact excitation of (a) the $^1\Pi$ State; (b) the $^1\Sigma^+$ State. See text for further details.

agreement with previous data (see Refs. 10 and 17 and references therein). These bands are reported with a maximum absolute cross section of 0.3, 32.3, and 329.2 Mb, respectively. In Figure 2, a small feature discernible at ~6.25 eV is due to a small $CS_2$ contamination that does not interfere at all with the assignments and fine structure observed other than in the 6.0–6.5 eV COS absorption spectrum. This corresponds to the $^1\Sigma_u^+$ most intense excitation band of $CS_2$ and we have determined an impurity presence of just 0.04%.

The weakest absorption band is due to the dipole forbidden excitation in the $^1\Delta \leftarrow {}^1\Sigma^+$ transition, peaking at 5.506 eV where two vibrational progressions have been assigned

TABLE VI. Energies (eV) and oscillator strengths for $^1\Pi$, nsσ, and $^1\Sigma^+$ states of COS.

| State | Energy (eV) | Present photoabsorption | Present EELS | Feng *et al.*[10] | Rabalais *et al.*[36] |
|---|---|---|---|---|---|
| $^1\Pi$ | ~7.38 | 0.131 09 | 0.136 | 0.13 | 0.13 |
| nsσ | (7.842) | (0.040 61) | (0.0461) | (0.033 05) | |
| $^1\Sigma^+$ | 7.920 | 0.068 64 | 0.0685 | 0.094 14 | … |
| | 8.025 | 0.104 30 | 0.1090 | 0.111 41 | … |
| | 8.130 | 0.120 41 | 0.1211 | 0.120 17 | … |
| | 8.224 | 0.095 80 | 0.1050 | 0.103 73 | … |
| | 8.321 | 0.072 90 | 0.0761 | 0.067 88 | … |
| | 8.417 | 0.040 62 | 0.0482 | 0.042 69 | … |
| | 8.510 | 0.024 07 | 0.0252 | 0.019 10 | … |
| | 8.595 | 0.009 66 | 0.0131 | 0.007 04 | … |
| | 8.664 | 0.004 47 | 0.0085 | 0.001 38 | … |
| | Sum | 0.581 47 | 0.6208 | 0.600 59 | 0.38 |

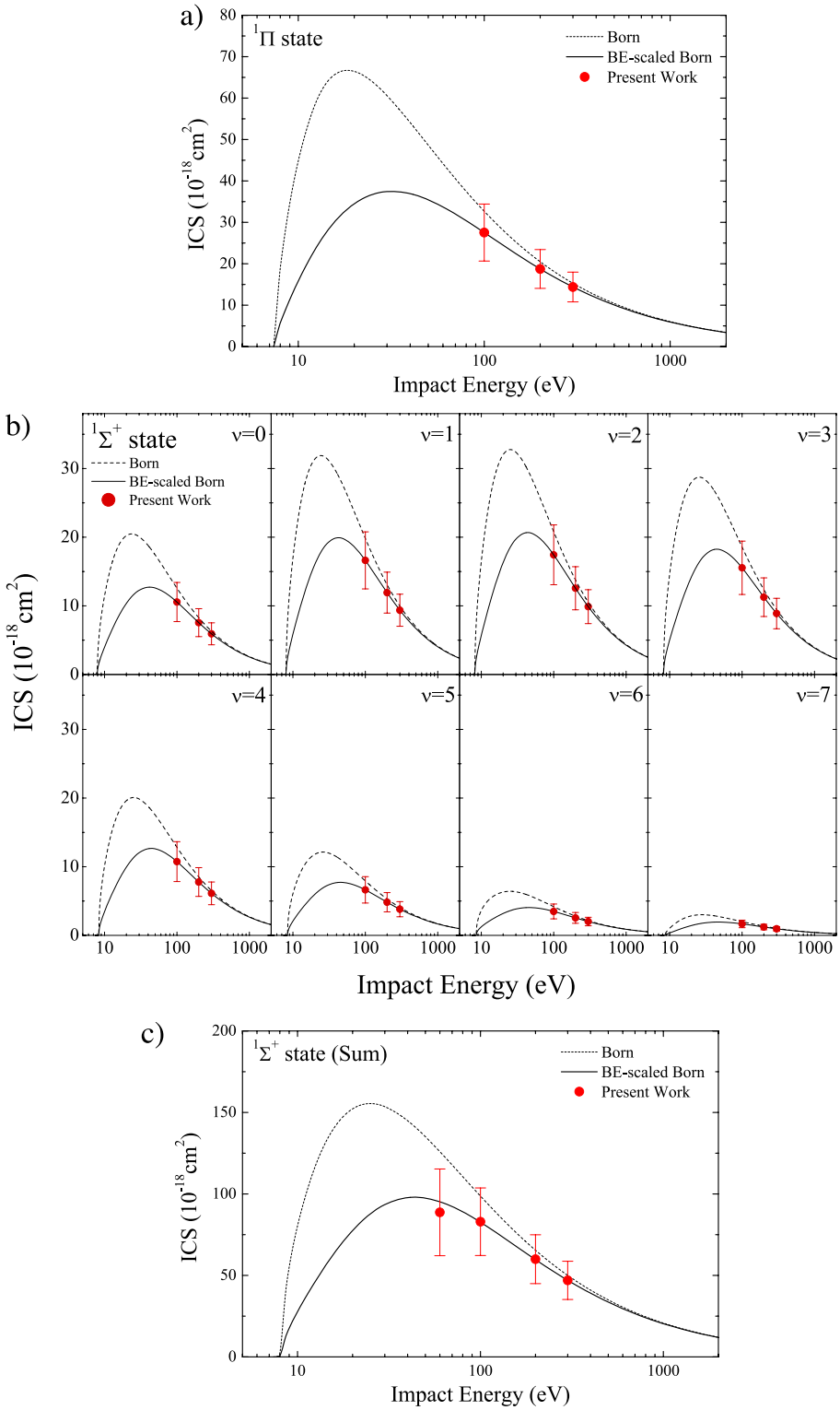


FIG. 8. Integral cross sections ($10^{-18}$ cm$^2$) of COS electron impact excitation for the (a) $(3\pi \rightarrow 10\sigma)^1\Pi$ transition; (b) $(3\pi \rightarrow 4\pi)^1\Sigma^+$ transition; (c) $(3\pi \rightarrow 4\pi)^1\Sigma^+$ transition (sum). See text for further details.

(Figure 2). Such vibronic excitation with considerable change in geometry in the upper excited state may turn this band discernible. Such assumption seems plausible since OCS $\nu_2'$ bending mode is being excited (see below). Previously, we have observed a similar effect on acetone lowest-lying excited state dipole forbidden band, identified as $3b_1(\pi^*) \leftarrow 5b_2(n_y)$ ($1^1A_2 \leftarrow 1^1A_1$), due to change from $C_{2v}$ ground state to $C_S$ excited state symmetry.[34] The origin of the band has been identified at 5.297 eV[35] from temperature dependent experiments on carbonyl sulphide, whereas in the present work, we propose the (0–0) transition at 5.267 eV. The fine structure is primarily attributed to excitation of the $\nu_1'$ stretching mode (see Table I for the proposed assignments) with a contribution from $\nu_2'$ bending mode. This interpretation appears to be consistent with the comment of Wu *et al.*[35] From the present analysis, the mean vibrational excitation energies of mode $\nu_1'$ are 0.082 eV, 0.024 eV lower than its value in the electronic ground state, whereas $\nu_2'$ mean energy is 0.045 eV, in contrast to 0.064 eV in

the electronic ground state. The feature at 5.21(8) eV is here proposed as a $\nu_2'$ hot band in agreement with the 5.250 eV weak structure previously reported in Ref. 35. Of relevance the fact that the weak vibrational structure may be accompanied by an underlying continuum suggesting a pre-dissociation band. A detailed analysis of Figure 2 reveals that the slope of the band above ~5.80 eV shows a slightly difference from below this value. Such may suggest the presence of another electronic state contributing to the absorption characteristic. We also note a modest structure at ~5.80, ~5.86, and ~5.89 eV, which have been tentatively assigned to $1\nu_1'$, $1\nu_1' + 1\nu_2'$ and $2\nu_1'$, respectively. Schmidt and co-workers[12] reported extensive calculations on COS potential energy surfaces with two distinctive dissociative singlet states obtained at 5.82 and 5.73 eV and assigned to the $1^1\Delta$ and $1^1\Sigma^-$ states, respectively. Worth mentioning that excitation from the ground $^1\Sigma^+$ to the $^1\Sigma^-$ excited state is dipole forbidden,[18] yet the calculation shows that in the $C_S$ symmetry, the excited $1^1\Delta$ and $1^1\Sigma^-$ states correlate with $2^1A'$ and $1^1A''$, respectively. Moreover, they calculated the vibrational excitation energies of $\nu_1'$ and $\nu_2'$ which are in good agreement with the values obtained in the energy spacing of the tentative assignment (0.090 and 0.060 eV, respectively). As so, the present data show for the first time experimental evidence of possible states contribution at ~5.80 eV. Hitherto, this would benefit from extensive electron energy loss measurements and different levels of theory calculations which are beyond the scope of the present contribution.

The VUV spectrum in Figure 3 (6.5–7.8 eV) presents a high-resolution analysis of the optically allowed transition ($10\sigma \leftarrow 3\pi$) ($^1\Pi \leftarrow {}^1\Sigma^+$) peaking at 7.458 eV. This transition appears with two long vibrational progressions, here clearly resolved for the first time. We tentatively proposed the origin (0–0) of this transition to lie at 6.57(4) eV. These are due to the excitation of $\nu_2'$ bending mode with mean values of the vibrational quanta of 0.064 eV (Table II). Such vibronic excitation separates the $^1\Pi$ state in the $^1A'$ and $^1A''$ components of the $C_S$ symmetry excited state, as previously reported by Rabalais *et al.*[36] and Leclerc and co-workers.[17]

Figure 4 shows the COS VUV photoabsorption band in the 7.7–8.7 eV region which is by far the dominant optically allowed transition and is assigned to ($4\pi \leftarrow 3\pi$) ($^1\Sigma^+ \leftarrow {}^1\Sigma^+$). The features observed in this energy region are generally speaking well-resolved with the exception of the low energy. The fine structure is mainly assigned to progression of the symmetric stretching vibration ($\nu_1'$), with mean energy of 0.098 eV, coupled with $\nu_2'$ bending mode (Table III). Leclerc *et al.*[17] have suggested that another progression previously identified by Matsunaga and Watanabe[37] was due to excitation of an underlying state assigned as ($11\sigma$) $^1\Pi$, which according to Ref. 17 contributes to the asymmetry of the $^1\Sigma^+$ band on the low energy side. We believe those authors meant the shoulder structures clearly visible in the left side of the features at 8.025 and 8.130 eV, which in Figure 4 we have assigned to a modest progression with 0.105 eV spacing and due to $\nu_1'$ symmetric stretching mode being active. The subject related to the valence and/or Rydberg character of the $^1\Sigma^+$ state has been thoroughly discussed by Leclerc *et al.*,[17] and we propose in Table VII a concise assignment for the Rydberg series converging to ionic electronic ground states $\tilde{X}\,^2\Pi_{3/2,1/2}$ of COS (see Sec. V B).

The absorption region from 8.7 to 10.8 eV is densely populated with several vibrational progressions (Tables IV and V), some of which superimposed on Rydberg series. We have followed the assignments made by Leclerc *et al.*[17] and identify three distinct electronic states $\tilde{E}\,^1\Pi$, $\tilde{F}\,^1\Pi$, and $\tilde{P}\,^1\Pi$ at 8.787, 8.850, and 9.017 eV, respectively, combined with vibrational quanta of mainly two modes (Table IV) composed of the symmetric, $\nu_1'$, and asymmetric, $\nu_3'$, stretching vibrations. The latter state ($\tilde{P}\,^1\Pi$) also accommodates a Rydberg series converging to the $\tilde{X}\,^2\Pi_{3/2}\,COS^+$ (see below). A weak contribution from $\nu_2'$ bending mode is also discernible in the 8.850–9.519 eV energy region. Thus, the vibrations involved show average values of 0.085, 0.045, and 0.248 eV, for $\nu_1'$, $\nu_2'$, and $\nu_3'$, respectively. Notwithstanding, such an assignment is still a difficult task, owing to vibronic interactions associated with closely spaced singlet excited states and to the presence of strong Fermi resonances.

### B. Rydberg transitions

The VUV spectrum above 7.8 eV consists of structures from Rydberg transitions (superimposed on absorption features) extending to the lowest IEs, which are here reported for the first time. The IE values of Wang *et al.*[13] are used to estimate the Rydberg series. The proposed Rydberg structures have not been labelled in the figures in order to avoid congestion and are listed in Table VII. The peak positions have been compared with the Rydberg formula: $E_n = E_i - R/(n-\delta)^2$, where $E_i$ is the ionisation energy (of the $\tilde{X}\,^2\Pi$ state), $n$ is the principal quantum number of the Rydberg orbital of energy $E_n$, $R$ is the Rydberg constant (13.61 eV), and $\delta$ (= n−n*) the quantum defect resulting from the penetration of the Rydberg orbital into the core. In addition to the values listed in Table VII, we have compared our data with other authors where available.

Using 11.183 and 11.229 eV as the ionisation limits, we clearly identify four series for each limit. For the $\tilde{X}\,^2\Pi_{3/2}$ state, the first member appears as a shoulder at 7.85(2) eV in the low-energy side of the $^1\Sigma^+$ band and is assigned to ($ns\sigma \leftarrow 3\pi$) ($11\sigma \leftarrow 3\pi$),[17] whereas the second at 9.667 eV is accompanied by vibrational progressions analysed above, with frequency values of the same order as those of the $\tilde{X}\,^2\Pi$ state of $COS^+$.[13] For the Rydberg series $np\sigma$ and $nd\sigma$, we note a few members with quite high quantum defects, which may be attributed to their broad nature and/or superposition with members of other Rydberg series. The next members of the other series also present vibrational progressions (Figure 5 and Tables III–V). The feature at 9.017 eV is assigned to the first member of an $nd\sigma$ series which is superimposed on the valence $\tilde{P}\,^1\Pi$ (see above).

As far as the $\tilde{X}\,^2\Pi_{1/2}$ state is concerned, the first member appears at 8.025 eV whereas the feature at 10.647 eV shows a considerable high quantum defect for an $ns$ series. The higher members of these Rydberg series, for which the relative intensity decreases, are difficult to assign due to overlap with other transitions and possible vibronic structure.

### C. BE-*f* scaling

The experimental GOS for the optically allowed transitions ($^1\Sigma^+$ and $^1\Pi$) is derived from the DCS at 60, 100, 200, and

TABLE VII. Energies (eV) and effective quantum numbers (n*) for Rydberg series converging to ionic electronic ground states $\tilde{X}\,^2\Pi_{3/2,1/2}$ of COS.

| Vertical energy | n* | Assignment | Reference 17 | n* | Reference 14 | Assignment |
|---|---|---|---|---|---|---|
| IE = 11.183 eV | | | | | | |
| | | | nsσ ← 3π | | | |
| 7.85(2) (b) | 2.02 | 3 | 7.86 | 2.03 | 7.767[a] | 4sσ |
| 9.667 | 3.00 | 4 | 9.672 | 3.01 | 9.235[a] | 5sσ |
| 10.341 | 4.02 | 5 | 10.328 | 4.01 | 10.137[a] | 6sσ |
| 10.647 | 5.04 | 6 | 10.656 | 5.12 | 10.527[a] | 7sσ |
| | | | npσ ← 3π | | | |
| 8.520 | 2.26 | 3 | 8.509 | 2.26 | ... | ... |
| 9.883 | 3.24 | 4 | 9.884 | 3.25 | 9.224 | 4pσ |
| 10.441 | 4.28 | 5 | 10.424 | 4.26 | 9.990[a] | 5pσ |
| 10.64(7) (b) | 5.04 | 6 | 10.700 | 5.36 | 10.486[a] | 6pσ |
| | | | ndσ ← 3π | | | |
| 9.017 | 2.51 | 3 | 9.024 | 2.51 | 9.651[a] | 3dσ |
| 10.105 | 3.55 | 4 | 10.116 | 3.59 | 10.324[a] | 4dσ |
| 10.529 | 4.56 | 5 | 10.536 | 4.62 | 10.635[a] | 5dσ |
| 10.767 | 5.71 | 6 | 10.740 | 5.60 | 10.787 | 6dσ |
| | | | ndπ ← 3π | | | |
| 9.578 | 2.91 | 3 | 9.584 | 2.93 | 9.690 | 3dπ |
| 10.302 | 3.93 | 4 | 10.252 | 3.84 | 10.329 | 4dπ |
| 10.620 | 4.97 | 5 | 10.584/10.604 | 4.81 | 10.650 | 5dπ |
| 10.767 | 5.72 | 6 | 10.772 | 5.82 | 10.825 | 6dπ |
| IE = 11.229 eV | | | | | | |
| | | | nsσ ← 3π | | | |
| 8.025 | 2.06 | 3 | 8.852 | 2.42 | 7.952[a] | 4sσ |
| 9.755 | 3.04 | 4 | 10.024 | 3.44 | 9.579[a] | 5sσ |
| 10.388 | 4.02 | 5 | 10.490 | 4.46 | 10.239[a] | 6sσ |
| 10.647 | 4.84 | 6 | 10.729 | 5.53 | 10.573[a] | 7sσ |
| | | | npσ ← 3π | | | |
| 8.664 | 2.30 | 3 | ... | ... | | |
| 9.98(3) (w) | 3.30 | 4 | ... | ... | 8.857 | 4pσ |
| 10.485 | 4.28 | 5 | ... | ... | 10.073 | 5pσ |
| 10.767 | 5.43 | 6 | ... | ... | 10.540 | 6pσ |
| | | | ndσ ← 3π | | | |
| 8.942 | 2.44 | 3 | ... | ... | 9.647 | 3dσ |
| 10.064 | 3.42 | 4 | ... | ... | 10.364 | 4dσ |
| 10.529 | 4.41 | 5 | ... | ... | 10.663 | 5dσ |
| 10.767 | 5.43 | 6 | ... | ... | 10.838 | 6dσ |
| | | | ndπ ← 3π | | | |
| 9.641 | 2.93 | 3 | ... | ... | 9.826[a] | 3dπ |
| 10.341/10.354 | 3.91/3.94 | 4 | ... | ... | 10.429[a] | 4dπ |
| 10.647 | 4.84 | 5 | ... | ... | 10.710[a] | 5dπ |

[a]Calculated vertical values: (b) indicates a broad structure; (w) weak structure (the last decimal of the energy value is given in brackets for these less-resolved features).

300 eV for the forward scattering angles from 2° to 20° in steps of 1°. Note that absolute DCSs for 5° to 20° at 60 eV were used to normalize the relative DCSs reported previously[17] for 5° to 70° in Figure 9. The scattering angle was calibrated by using the $2^1$P DCS of He. For the $^1\Sigma^+$ state, the vibrational progression was decomposed from $v = 1$ to $v = 7$ by Gaussian fitting. For the $^1\Pi$ state, though fine structures are clearly observed, those were considered as one broad band centred at 7.4 eV due to instrumental resolution of the present electron impact spectrometer. As expected, all data are aligned on the universal curve within the error bars, reaching $f_0$ along $\Delta K \rightarrow 0$ under the Lassettre limit theorem[29] (Figures 7(a) and 7(b)). Relative and absolute oscillator strengths are tabulated in Table VI for the vibronic states of the $^1\Pi$, ns$\sigma$, and $^1\Sigma^+$. The present absolute photoabsorption cross sections are converted to differential absolute optical oscillator strengths, viz., σ (Mb) = 1.0975 × $10^2$ (d$f$/dE) ($eV^{-1}$), which are integrated to obtain the optical oscillator strengths for $^1\Pi$. The vibrational progressions of the $^1\Sigma^+$ sate are fitted with Lorentzian functions. A comparison of the $f_0$ value with the photoabsorption data is another assessment for verification and validation of the present measurements (Table VI). The present results show that the absolute $f_0$ values are much the same for the photoabsorption and the electron impact data. For the $^1\Pi$ transition, our present data are

in good agreement with the oscillator strength (0.130) reported from Brion and co-workers[10] and Rabalais *et al.*,[36] whereas for the $^1\Sigma^+$ transition, good agreement between the present OOSs and Brion's results is observed for the vibrational progressions from $v = 0$ to 7. Consequently, the integral OOS for the $^1\Sigma^+$ band agrees well with the value of 0.601 by Brion and co-workers[10] which is, however, 60% higher in intensity than the value of 0.38 derived from the photoabsorption of Rabalais *et al.*[36] Note that Chan *et al.*[38] stated that this discrepancy is due to experimental conditions (bandwidth/line width interaction) related probably to Beer-Lambert law line-saturation, particularly for narrow and intense discrete absorption peaks, leading to a lower measured cross section. However, these problems do not arise in the electron-impact spectra.

Along with our program to verify the BE$f$-scaling for atoms and molecules, in addition, ICSs were determined by extrapolating COS DCSs from 0° to 180° (not shown here) again using the Vriens[28] formula (3). Here, the Born ICS curve is derived from the apparent Born DCS (displayed as the dotted line in Figures 8(a) and 8(b)) at an impact energy of 300 eV. Then, the scaled Born ICS curve using Eq. (9) is shown in Figures 8(a) and 8(b) as the solid line. Figure 8(c) shows the ICS for the sum of $v = 1$ to $v = 7$. The present ICS data at 60, 100, and 200 eV are also largely consistent, within our stated uncertainties and with our own BE$f$-scaling computation. However, no experimental or theoretical data are available in the literature for comparison with the present results below 60 eV. Hence, one can say that we predict the ICSs for the intense optically allowed $^1\Pi$ and $^1\Sigma^+$ transitions in the intermediate energy region from threshold up to 100 eV. However, as observed in the high-resolution photoabsorption spectrum, the $^1\Sigma^+$ state is overlapped with other vibrational progression as well as with the Rydberg-valence state of s$\sigma$ with which the BE$f$-scaling approach may has its own limits of applicability, as is found in the longest band of $O_2$.[39] Furthermore, the contribution of strong Rydberg-valence mixing affecting the $^1\Pi$ state may certainly be a general limitation in the BE$f$-scaling approach. These verifications await further investigations, both experimental and theoretical in the intermediate energy region below 60 eV.

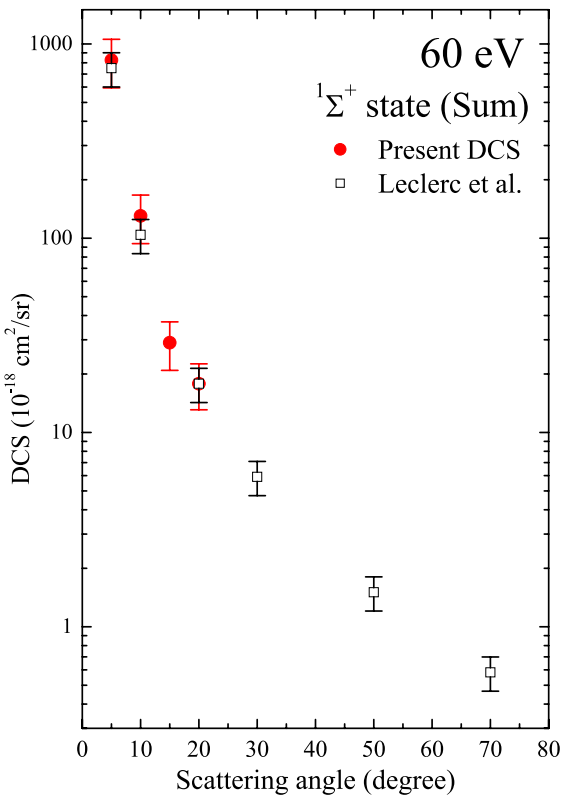


FIG. 9. Differential cross sections ($10^{-18}$ cm$^2$/sr) for vibrational sum of $^1\Sigma^+$ transition obtained from present EELS data at an impact energy of 60 eV together with relative DCS of Leclerc *et al.*[17] (normalized to present DCS at 20°).

### D. Absolute photoabsorption cross sections and atmospheric photolysis

The present optical measurements were carried out in the pressure range of 0.02–0.98 Torr and reveal no evidence for changes in absolute cross sections or peak energies as a function of pressure, thus we believe the present spectra are free of any saturation effects. Previous absolute VUV photoabsorption cross sections of COS are available in the wavelength ranges of 250–124 nm (5.0–10.0 eV),[36] 260–200 nm (4.8–6.2 eV),[35] and 170–107 nm (7.3–11.6 eV).[37] The present absolute cross section values are in good agreement with Wu *et al.*[35] at 5.506 eV and Matsunaga and Watanabe[37] at 7.458 eV, whereas at 7.458 eV, the value of Rabalais *et al.*[36] is only half of our present 32.3 Mb value. When comparing the present data (Figure 1) with the high energy electron impact (the pseudo photon) technique of Feng *et al.*,[10] each set has been convoluted with a Gaussian function of 0.05 eV and they are displayed as the red-line in Figure 6. Meanwhile, the photoabsorption data from Rabalais *et al.*[36] and Matsunaga and Watanabe[37] were also convoluted (not shown in Figure 6) and we observe that our synchrotron radiation results agree quite well with the pseudo photon data of Feng *et al.*[10] Consequently, we may be confident that the present photoabsorption data are not subject to line-saturation effects. In addition, the agreement of previous cross sections measured at the ASTRID beamline with the most precise data available in the literature (see Eden *et al.*[40] and references therein) indicates that the present carbonyl sulphide cross sections can be relied upon across the energy range studied (4.0–10.8 eV). Note, though within the error bars, discrepancies in magnitude change systematically with the photon energy between the present and the pseudo photon data.

The present absolute cross sections below 6.89 eV (above 180 nm) can be used in combination with solar actinic flux[41] measurements available from the literature to estimate the photolysis rate of OCS in the atmosphere from an altitude close to the ground to the stratopause at 50 km. Details of the calculation programme are presented by Limão-Vieira *et al.*[42] in which the quantum yield for dissociation following absorption is assumed to be unity. The reciprocal of the photolysis rate at a given altitude corresponds to the local photolysis lifetime. Photolysis lifetimes of less than 10 sunlit days were calculated at altitudes above 15 km with less than a day above 30 km. This shows that carbonyl sulphide molecules can be broken up quite efficiently by UV absorption at these altitudes.

From the ground level up to the tropopause, the lifetimes are so low (<20 days) that photolysis may be a relevant sink mechanism.

A recent quantum chemical and theoretical kinetics study on the reaction of COS with H, OH, and O ($^3$P)[43] (and references therein) have shown that the fastest chemical sink reaction which may have atmospheric implications is with the hydrogen atom. Whether this mechanism is prevalent in detriment to photolysis is still not known precisely and so UV photolysis may play a significant role in removing carbonyl sulphide from the terrestrial atmosphere.

## VI. CONCLUSIONS

The present work provides the first complete study of the VUV electronic spectroscopy of COS and provides the most reliable set of absolute photoabsorption cross sections between 4.0 and 10.8 eV to date. The dense and extensive vibrational progressions of the $(4\pi)^1\Delta$ state at around 5.267 eV and $(10\sigma)$ $^1\Pi$ state at 6.57(4) eV were resolved and analysed for the first time by high-resolution VUV photoabsorption, whilst a new $^1\Sigma^-$ state is proposed for the first time. The most intense absorption band assigned to $(4\pi \leftarrow 3\pi)$ ($^1\Sigma^+ \leftarrow {}^1\Sigma^+$) was revisited with new features identified. Mixed valence-Rydberg character is observed in particular for the low-lying members of *np* and *ns* series, with bond stretching and bond bending in the corresponding excited states. Thus, with the present high resolution data, it is possible to theoretically analyse the associated vibrational progressions and determine the vibration quanta involved. The Rydberg series have been established and some previously reported using the high-resolution electron impact technique[17] are confirmed in the present experiment. Absolute oscillator strengths are determined from the differential OOSs for the $^1\Sigma^+$ and $^1\Pi$ states and found to agree with previous data obtained from pseudo photon experiments conducted using 1.5 keV electrons. These OOSs are also in accord with those obtained from the present EELS data by using the Lassettre limit theorem. Furthermore, by using the BE$f$-scaling method, ICSs are provided for the first time for the $^1\Sigma^+$ and $^1\Pi$ states in the intermediate impact energy region.

The photolysis lifetimes of carbonyl sulphide have also been carefully derived for the Earth's troposphere and stratosphere and it is shown that solar photolysis may be a relevant sink in the terrestrial atmosphere.

## ACKNOWLEDGMENTS

F.F.S. and D.A. acknowledge post-doctoral Grant Nos. SFRH/BPD/68979/2010 and SFRH/BPD/99261/2013, respectively, and together with P.L.V. partial funding from the research Grant Nos. PEst-OE/FIS/UI0068/2014 and PTDC/FIS-ATO/1832/2012 through the Portuguese Foundation for Science and Technology, FCT-MEC. P.L.V. acknowledges his Visiting Professor positions at The Open University, UK and Sophia University, Tokyo, Japan and together with NJM the support from the British Council for the Portuguese-English joint collaboration. The authors wish to acknowledge the beam time at the ISA synchrotron at University of Aarhus, Denmark. We also acknowledge the financial support provided by the I3 Integrated Activity on Synchrotron and Free Electron Laser Science (IA-SFS), Contract No. RII3-CT-2004-506008, under the Research Infrastructure Action of the FP6 EC programme Structuring the European Research Area.

[1]R. J. Charlson, S. E. Schwartz, J. M. Hales, R. D. Cess, J. A. Coakley, J. E. Hansen, and D. J. Hofmann, "Climate forcing by anthropogenic aerosols," Science **225**, 423–430 (1992).

[2]P. Limão-Vieira, S. Eden, P. A. Kendall, N. J. Mason, and S. V. Hoffmann, "High resolution VUV photo-absorption cross-section for dimethylsulphide, $(CH_3)_2S$," Chem. Phys. Lett. **366**, 343-349 (2002).

[3]E. A. Drage, P. Cahillane, S. V. Hoffmann, N. J. Mason, and P. Limão-Vieira, "High resolution VUV photoabsorption cross section of dimethyl sulphoxide $(CH_3)_2SO$," Chem. Phys. **331**, 447–452 (2007).

[4]N. J. Mason, A. Dawes, R. Mukerji, E. A. Drage, E. Vasekova, S. M. Webb, and P. Limão-Vieira, "Atmospheric chemistry with synchrotron radiation," J. Phys. B: At., Mol. Opt. Phys. **38**, S893–S911 (2005).

[5]E. Kjellstrom, "A three-dimensional global model study of carbonyl sulfide in the troposphere and the lower stratosphere," J. Atmos. Chem. **29**, 151–177 (1998) and references therein.

[6]T. S. Bates, B. K. Lamb, A. Guenther, J. Dignon, and R. E. Stoiber, "Sulfur emissions to the atmosphere from natural sources," J. Atmos. Chem. **14**, 315–337 (1992) and references therein.

[7]B. C. Nguyen, N. Mihalopoulos, J. P. Putaud, and B. Bonsang, "Carbonyl sulfide emissions from biomass burning in the tropics," J. Atmos. Chem. **22**, 55–65 (1995) and references therein.

[8]M. E. Palumbo, T. R. Geballe, and A. G. G. M. Tielens, "Solid carbonyl sulfide (OCS) in dense molecular clouds," Astrophys. J. **479**, 839–844 (1997).

[9]E. Lellouch, G. Paubert, R. Moreno, M. Festou, B. Bezard, D. Bockelee-Morven, P. Colom, J. Crovisier, T. Encrenaz, D Gautier *et al.*, "Chemical and thermal responde of jupiter atmosphere following the impact of comet shoemaker-levy-9," Nature **373**, 592–595 (1995).

[10]R. Feng, G. Cooper, and C. E. Brion, "Quantitative studies of the photoabsorption of carbonyl sulphide in the valence-shell, S 2p, 2s and C1s inner-shell regions (4-360 eV) by dipole electron impact spectroscopies," Chem. Phys. **252**, 359–378 (2000) and references therein.

[11]S. E. Wheeler, A. C. Simmonett, and H. F. Schaefer, "Theoretical calculations on the renner-teller bending frequencies of the $\tilde{A}\ ^2\Pi$ state of $OCS^+$," J. Phys. Chem. A **111**, 4551–4555 (2007).

[12]J. A. Schmidt, M. S. Johnson, G. C. McBane, and R. Schinke, "The ultraviolet spectrum of OCS from first principles: Electronic transitions, vibrational structure and temperature dependence," J. Chem. Phys. **137**, 054313 (2012).

[13]L.-S. Wang, J. E. Reutt, Y. T. Lee, and D. A. Shirley, "High resolution UV photoelectron spectroscopy of $CO_2^+$, $COS^+$ and $CS_2^+$ using supersonic molecular beams," J. Electron Spectrosc. Relat. Phenom. **47**, 167–186 (1998).

[14]C. Cossart-Magos, M. Jungen, R. Xu, and F. Launay, "High resolution absorption spectrum of jet-cooled OCS between 64000 and 91000 $cm^{-1}$," J. Chem. Phys. **119**, 3219–3233 (2003).

[15]H. Murai, Y. Ishijima, T. Mitsumura, Y. Sakamoto, H. Kato, M. Hoshino, F. Blanco, G. García, P. Limão-Vieira, M. J. Brunger, S. J. Buckman, and H. Tanaka, "A comprehensive and comparative study of elastic electron scattering from OCS and $CS_2$ in the energy region from 1.2 to 200 eV," J. Chem. Phys. **138**, 054302 (2013).

[16]W. M. Flicker, O. A. Mosher, and A. Kuppermann, "Electron-impact excitation of low-lying electronic states in $CS_2$, OCS, and SO," J. Chem. Phys. **69**, 3910 (1978).

[17]B. Leclerc, A. Poulin, D. Roy, M.-J. Hubin-Franskin, and J. Delwiche, "Study of OCS by electron energy loss spectroscopy," J. Chem. Phys. **75**, 5329–5348 (1981).

[18]G. Herzberg, *Molecular Spectra and Molecular Structure III. Electronic Spectra and Electronic Structure of PolyatomicMolecules* (Van Nostrand, Princeton, 1966).

[19]S. Eden, P. Limão-Vieira, S. V. Hoffmann, and N. J. Mason, "VUV photoabsorption in $CF_3$ X (X = Cl, Br, I) fluoro-alkanes," Chem. Phys. **323**, 313–333 (2006).

[20]H. Tanaka, L. Boesten, D. Matsunaga, and T. Kudo, "Differential elastic electron scattering cross sections for ethane in the energy range from 2 to 100 eV," J. Phys. B: At., Mol. Opt. Phys. **21**, 1255–1263 (1988).

[21]H. Tanaka, T. Ishikawa, T. Masai, T. Sagara, L. Boesten, M. Takekawa, Y. Itikawa, and M. Kimura, "Elastic collisions of low-to intermediate-energy electrons from carbon dioxide: Experimental and theoretical differential cross sections," Phys. Rev. A **57**, 1798–1808 (1998).
[22]H. Kato, T. Asahina, H. Masui, M. Hoshino, H. Tanaka, H. Cho, O. Ingolfsson, F. Blanco, G. García, S. J. Buckam, and M. J. Brunger, "Substitution effects in elastic electron collisions with $CH_3X$ (X=F, Cl, Br, I) molecules," J. Chem. Phys. **132**, 074309 (2010).
[23]L. Boesten and H. Tanaka, "Rational function fits to the nonresonant elastic differential cross sections (DCS) for e + He collisions, 0°–180°, 0.1 to 1000 eV," At. Data Nucl. Data Tables **52**, 25–42 (1992).
[24]S. K. Srivastava, A. Chutjian, and S. Trajmar, "Absolute elastic differential electron scattering cross sections in the intermediate energy region. I. $H_2$," J. Chem. Phys. **63**, 2659–2665 (1975).
[25]R. T. Brinkmann and S. Trajmar, "Effective path length corrections in beam-beam scattering experiments," J. Phys. E: Sci. Instrum. **14**, 245–255 (1981).
[26]J. C. Nickel, P. W. Zetner, G. Shen, and S. Trajmar, "Principles and procedures for determining absolute differential electron-molecule (atom) scattering cross sections," J. Phys. E: Sci. Instrum. **22**, 730–738 (1989).
[27]Y.-K. Kim, "Scaled born cross sections for excitations of $H_2$ by electron impact," J. Chem. Phys. **126**, 064305 (2007).
[28]L. Vriens, "Excitation of helium by electrons and protons," Phys. Rev. **160**, 100–108 (1967).
[29]E. N. Lassettre, A. Skerbele, and M. A. Dillon, "Generalized oscillator strength for $1^1S \rightarrow 2^1P$ transition of helium. Theory of limiting oscillator strengths," J. Chem. Phys. **50**, 1829 (1969).
[30]B. H. Bransden and C. J. Joachain, *Physics of Atoms and Molecules* (Longmans, London, 1983).
[31]Y.-K. Kim, "Scaling of plane-wave born cross sections for electron-impact excitation of neutral atoms," Phys. Rev. A **64**, 032713 (2001).
[32]K. Anzai, H. Kato, M. Hoshino, H. Tanaka, Y. Itikawa, L. Campbell, M. J. Brunger, S. J. Buckman, H. Cho, F. Blanco, G. García, P. Limão-Vieira, and O. Ingólfsson, "Cross section data sets for electron collisions with $H_2$, $O_2$, CO, $CO_2$, $N_2$ O and $H_2$ O," Eur. Phys. J. D **66**, 36 (2012).
[33]D. Duflot, M. Hoshino, P. Limão-Vieira, A. Suga, H. Kato, and H. Tanaka, "$BF_3$ valence and Rydberg states as probed by electron energy loss spectroscopy and *ab initio* calculations," J. Phys. Chem. A **118**, 10955-10966 (2014).
[34]M. Nobre, A. Fernandes, F. F. da Silva, R. Antunes, D. Almeida, V. Kokhan, S. V. Hoffmann, N. J. Mason, S. Eden, and P. Limão-Vieira, "The VUV electronic spectroscopy of acetone studied by synchrotron radiation," Phys. Chem. Chem. Phys. **10**, 550–560 (2008).
[35]C. Y. R. Wu., F. Z. Chen, and D. L. Judge, "Temperature-dependent photoabsorption cross sections of OCS in the 200–260 nm," J. Quant. Spectrosc. Radiat. Transfer **61**, 265–271 (1999).
[36]J. W. Rabalais, J. M. McDonald, V. Scherr, and S. P. McGlynn, "Electronic spectroscopy of isoelectronic molecules. II. Linear triatomic groupings containing sixteen valence electrons," Chem. Rev. **71**, 73–108 (1971).
[37]F. M. Matsunaga and K. Watanabe, "Ionization potential and absorption coefficient of COS," J. Chem. Phys. **46**, 4457–4459 (1967).
[38]W. F. Chan, G. Cooper, and C. E. Brion, "Absolute optical oscillator-strengths for the electronic excitation of atoms at high-resolution–experimental methods and measurements for helium," Phys. Rev. A **44**, 186-204 (1991).
[39]D. Suzuki, H. Kato, M. Ohkawa, K. Anzai, H. Tanaka, P. Limão-Vieira, L. Campbell, and M. J. Brunger, "Electron excitation of the Schumann–Runge continuum, longest band, and second band electronic states in $O_2$," J. Chem. Phys. **134**, 064311 (2011).
[40]S. Eden, P. Limão-Vieira, S. V. Hoffmann, and N. J. Mason, "VUV spectroscopy of $CH_3Cl$ and $CH_3I$," Chem. Phys. **331**, 232-244 (2007).
[41]Chemical Kinetics and Photochemical Data for Use in Stratospheric Modelling, Evaluation number 12, NASA, Jet Propulsion Laboratory, JPL Publication 97–94, January 15, 1997.
[42]P. Limão-Vieira, S. Eden, P. A. Kendall, N. J. Mason, and S. V. Hoffmann, "VUV photo-absorption cross-section for $CCl_2F_2$," Chem. Phys. Lett. **364**, 535–541 (2002).
[43]V. Saheb, M. Alizadeh, F. Rezaei, and S. Shahidi, "Quantum chemical and theoretical kinetics studies on the reaction of carbonyl sulfide with H, OH and O (3P)," Comput. Theo. Chem. **994**, 25–33 (2012).